High-Strength Hemicellulose-based Conductive Composite Hydrogels Reinforced by Hofmeister Effect

Zejiang Guo,* Yuxuan Fang, and Zhenyu Wang

Hemicellulose is a renewable and environmentally friendly biomass polysaccharide. However, because of the low polymerization degree, conventional hemicellulose-based hydrogels often have poor mechanical properties, severely restricting their potential applications. This study involved preparation of a novel high-strength conductive hemicellulose-based composite hydrogel, modulated by a Na_2SO_4 solution. The hydrogel matrix with a physicochemical double cross-linking structure was created by adding polyvinyl alcohol to the chemically crosslinked networks of gelatin and dialdehyde xylan (DAX) to improve the enhancing effect. After being soaked in a 1 M Na_2SO_4 solution for 24 h, the composite hydrogel's network structure was thicker, as revealed by scanning electron microscopy. Its tensile breaking strength (3.02 MPa) and elongation (330.95%) were much higher than those prior to the treatment. Energy dispersive spectroscopy and X-ray diffraction confirmed that the composite hydrogel had a considerable amount of Na^+ and SO_4^{2-} uniformly dispersed throughout. Additionally, the ionic conductivity of the composite hydrogel was measured at 5.4×10^{-3} S/m, indicating a potential use in the field of super-capacitors.

DOI: 10.15376/biores.19.4.7708-7722

Keywords: Hemicellulose; Hydrogels; Hofmeister effect; High strength; Conductive

*Contact information: Hubei Provincial Key Laboratory of Green Materials for Light Industry, Hubei University of Technology, Wuhan 430068, China; *Corresponding author: praecipua@126.com*

INTRODUCTION

Hemicelluloses are a type of alkali-soluble heteropolysaccharide found in plant cell walls, and in nature they are second only to cellulose (Gao *et al.* 2023; Rao *et al.* 2023). Hemicellulose has drawn a lot of interest in the realm of hydrogels because of its abundant source and superior biocompatibility. However, hemicellulose has a low degree of polymerisation and a complex structure with side groups, making the cross-linking of the hydrogel network sparse and poorly uniform (Fredricks *et al*. 2023). Therefore, the mechanical properties of conventional hemicellulose-based hydrogels are generally poor, which largely limits their practical applications.

Hydrogels are cross-linked hydrophilic polymeric materials with three-dimensional network structure; they are able to absorb large volumes of water without being destroyed. Hydrogel materials have found extensive application in the field of metal ions adsorption (Dou *et al.* 2022; Sarmah and Karak 2022; Elgueta *et al.* 2023), controlled drug release (Lacroce and Rossi 2022; Zhou *et al.* 2022; Li *et al.* 2023), tissue engineering (Lee and Mooney 2001; Gutiérrez Hernández *et al.* 2023; Yuan *et al.* 2023), biosensors (Jung *et al.* 2017; Hu *et al.* 2023; Pan *et al.* 2023), and supercapacitors (Gong *et al.* 2020; Mondal *et al.* 2022; Song *et al.* 2023), since the first reporting of poly(2-hydroxyethyl methacrylate)

hydrogels for contact lenses in 1960 (Wichterle and Lim 1960). However, due to the limitation of mechanical properties, hemicellulose-based hydrogels have achieved limited practical results in these applications.

To change this status quo, many strategies have been used for hydrogel preparation. Some of this work has achieved excellent mechanical properties, such as topological structure (Okumura and Ito 2001), double-network structure (Gong *et al.* 2003), dual-crosslinked structure (Li *et al.* 2022b), organic-inorganic nanocomposite structure (Haraguchi 2011), microphase separation structure (Ihsan *et al.* 2016), microcrystals structure (Lin *et al.* 2019), and their combinations. The hemicellulose molecular chain contains many reactive hydroxyl groups, which can significantly increase its molecular weight under the cross-linking effect of epichlorohydrin, thus making hemicellulose able to form more and tighter cross-linking structure in the process of gelation (Qi *et al.* 2016). By further compounding with other materials, through the construction of double network structure, double cross-linked structure, and organic-inorganic composite structure, hemicellulose-based hydrogels with satisfactory mechanical properties can be obtained (Sun *et al.* 2015; Ling *et al.* 2022; Wang *et al.* 2023). Despite various advances in toughening hemicellulose-based hydrogels by the above methods, their mechanical properties are still unsatisfactory when compared to anhydrous polymers or even to synthetic polymer hydrogels. In view of this, the introduction of microcrystalline structures into hemicellulose-based hydrogel networks may greatly improve their mechanical properties.

Microcrystalline structures have drawn interest in the field of hydrogels due to their high chain density and crystal domain disruption energy. Additionally, the creation of microcrystals effectively inhibits the extension of cracks (Zhao *et al.* 2021). This is due to the higher chain density and rupture energy of the crystalline domains, as well as the fact that the highly anisotropic microstructure is susceptible to crack deflection under loading (Li and Gong 2024). This somewhat offsets the detrimental impact of water molecules on the interactions between polymers. Freeze-thawing, solvent exchange, fast quenching, and salt-out are the general methods used to introduce microcrystalline structures into hydrogels (Li and Gong 2024). Salt-out and salt-in are two distinct approaches based on the Hofmeister effect. Different salts exhibit distinguishable abilities to precipitate proteins from aqueous solutions, which is known as the Hofmeister effect or ion-specific effect (Wu *et al.* 2021a). This impact is assumed to be caused by variations in the hydration capacity of ions. Through interacting with hydration water near hydrophilic functional groups on hydrophobic chains, ions during salting out enhance polymer intermolecular interactions and aid in the creation of microcrystals (Wu *et al.* 2021a). Currently, no reports have been seen on hemicellulose-based hydrogels in this regard. However, research on the mechanical properties of polyvinyl alcohol (PVOH) and gelatin-based hydrogels have substantially increased over the years through a simple salt solution soaking treatment (Li *et al.* 2022a; Zou *et al.* 2023). Cheng *et al.* (2023) and Yin *et al.* (2024) obtained PVOH/poly(acrylamide) double-network hydrogels with denser structure and higher crystallinity, whose tensile strength could be significantly increased from the initial kPa level to 18.9 MPa through the soaking treatment with citrate ions. Furthermore, Wu *et al.* (2021a) compared the critical gel concentration of 5 wt% PVOH under various ions and found that the anion's enhancing effect was greater than the cation's. Additionally, due to the diffusion of salt ions, the soaked hydrogels tend to have good ionic conductivity (Wu *et al.* 2021b; Cui *et al.* 2022), which will give them a certain application potential in the field of biosensors, supercapacitors, and other electronic devices.

In the present work, the authors selected SO_4^{2-}, $S_2O_3^{2-}$, $H_2PO_4^-$, CO_3^{2-}, CH_3COO^-, Cl^- and Li^+, Na^+, K^+, Ba^{2+}, Ca^{2+}, Fe^{3+} in the Hofmeister series. The effects of Hofmeister ions on the structure and properties of hemicellulose-based hydrogels were studied in detail by X-ray diffraction (XRD), energy dispersive spectrum (EDS), and electronic universal testing. In addition, based on the modulation mechanism, DAX-gelatin/PVOH physicochemical double cross-linked network conductive composite hydrogels were successfully prepared. To the best of the authors' knowledge, this is the first study to prepare hemicellulose-based hydrogels of high mechanical properties reinforced by Hofmeister Effect. The goal of this work was to explore the modulation mechanism of Hofmeister ions on hemicellulose-based hydrogels, and to provide a novel idea for the development of high strength hydrogels.

EXPERIMENTAL

Materials

Hemicellulose (HC) was extracted from corncob at 75 °C for 2 h using 10% KOH solution. Its xylose content of 75.1%, arabinose content of 15.4%, glucose content of 3.8%, and galactose content of 1.6% were measured by ion chromatography. Polyvinyl alcohol (PVOH, average polymerization degree 1750 ± 50, ⩾ 99%), was purchased from Sinopharm Chemical Reagent Co., Ltd. (Shanghai, China). Gelatin (240 Bloom) was purchased from Aladdin Industrial Corporation (Shanghai, China). Poly-vinylidene fluoride, acetylene black, and activated carbon were purchased from Jinghong New Energy Technology Co., Ltd. (Zhengzhou, China). Other chemical reagents were purchased from Sinopharm Chemical Reagent Co., Ltd. (Shanghai, China) and of analytical grade. All chemicals in this work were used without further treatment.

Methods

Preparation of dialdehyde xylan

Xylan was oxidized with sodium metaperiodate as previously reported (Amer *et al*. 2016). In brief, 2.50 g of xylan was suspended in sodium periodate solution (3.05 g in 500 mL of deionized water). The reaction was stirred at room temperature for 24 h. Using hydroxylamine hydrochloride potentiometric titration (Lee *et al*. 2020), the aldehyde group content of dialdehyde xylan was found to be 8.48 mmol/g. The product was dialyzed against deionized water for 48 h and then lyophilized for further characterization.

Preparation of composite hydrogels enhanced by Hofmeister effect

A total of 225 mg PVOH and 90 mg gelatin were added to 1 mL deionized water and stirred at 80 °C to dissolve them completely to obtain solution A. In addition, 60 mg DAX was added to 0.5 mL of deionized water and stirred at room temperature to obtain solution B. The solution A and B were mixed evenly and placed in the refrigerator at 4 °C for 4 h, and then removed at room temperature overnight to obtain the initial PVOH/gelatin-DAX (I-PGD) composite hydrogel. Finally, the I-PGD composite hydrogel was immersed 24 h in 40 mL 1 M Na_2SO_4 solution to obtain the conductive composite hydrogel enhanced by Hofmeister effect (H-PGD).

SEM Analysis

Morphology analysis of composite hydrogels (after freeze drying) in the cross-section was completed with imaging *via* Field Emission scanning electronic microscopy (SEM, SU8010, HITACHI Ltd., Tokyo, Japan) with a 3 kV accelerating voltage. To enhance the electric conductivity, the composite hydrogels were sprayed with gold using a magnetron ion sputter metal coating device (MSP-2S; IXRF Systems, Inc., Japan). Finally, the energy dispersive spectrum (EDS) mapping on the sample surface was characterized by a silicon drift detector equipped with SEM.

FT-IR Spectroscopy

Fourier transform-infrared spectra (Nicolet 6700 FT-IR, Thermo Fisher Scientific Inc., Waltham, MA, USA) was employed to obtain molecular information of DAX and composite hydrogels. The FT-IR spectra was recorded in the range 4000 to 400 cm^{-1}.

XRD Analysis

The crystallization structures of composite hydrogels were determined and collected by X-ray diffraction (XRD, Empyrean, PANalytical, Amsterdam, Netherlands) equipped with a CuKα (k = 1.54 A°) monochromatic radiation source with a wavelength of 0.154 nm, 45 kV operating tube voltage, and 40 mA tube current. All the diffracted intensities from 5° to 90° were recorded with a step size of 0.01° and a scanning speed of 5° min^{-1}. Then, the XRD patterns were presented after eliminating excess noise and removing the environmental background.

XPS Analysis

Surface chemical analysis of DAX samples was performed using an X-ray photoelectron spectrometer (PHI5000 Versaprobe III XPS, Physical Electronics, Inc., Chanhassen, MN, USA) equipped with Al Kα radiation as the excitation resource.

Mechanical property test

The compressive and tensile performance of composite hydrogel was evaluated using the electromechanical universal testing machine (CMT6103, Shenzhen SANS, China) with a 1000 N load cell at room temperature (25 °C) with relative humidity (50 % RH). The crosshead speed was set to be 50 mm/min and 10 mm/min in compressive and tensile test, respectively. All samples were tested at least three times.

Electrochemical performance analysis

The electrode materials were created by evenly applying a mixture of polyvinylidene fluoride, acetylene black, and activated carbon (7:2:1) on the aluminum foil surface. The electrodes were compounded with H-PGD composite hydrogel as the electrolyte ($20 \times 15 \times 1$ mm), the supercapacitor was built, and the electrochemical characteristics were assessed using a two-electrode system on an electrochemical workstation (Zennium Pro, Zahner, Germany). Additionally, electrochemical impedance spectroscopy (EIS) was used to determine the conductivity of the PGD composite hydrogel and cyclic voltammetric curve (CV), constant current charge discharge curve (GCD) were used to determine the electrode specific capacitance of the hydrogel capacitor (Tsay *et al.* 2012).

RESULTS AND DISCUSSION

Design of Composite Hydrogels

Figure 1 shows the general procedure for preparing the composite hydrogels with a physical-chemical double cross-linked network structure. The DAX and gelatin form a chemical cross-linking network *via* Schiff base reaction (Yu *et al*. 2023). The physical crosslinking network of PVOH, which is sensitive to salt solution, is also introduced. The PVOH molecule chains become entangled under the influence of SO_4^{2-}, tightening the hydrogel's structure and improving its mechanical qualities (Wu *et al.* 2021a). Furthermore, certain ionic conductivity properties of the composite hydrogel are also a result of the diffusion of salt ions in solution into the interior of the polymer network.

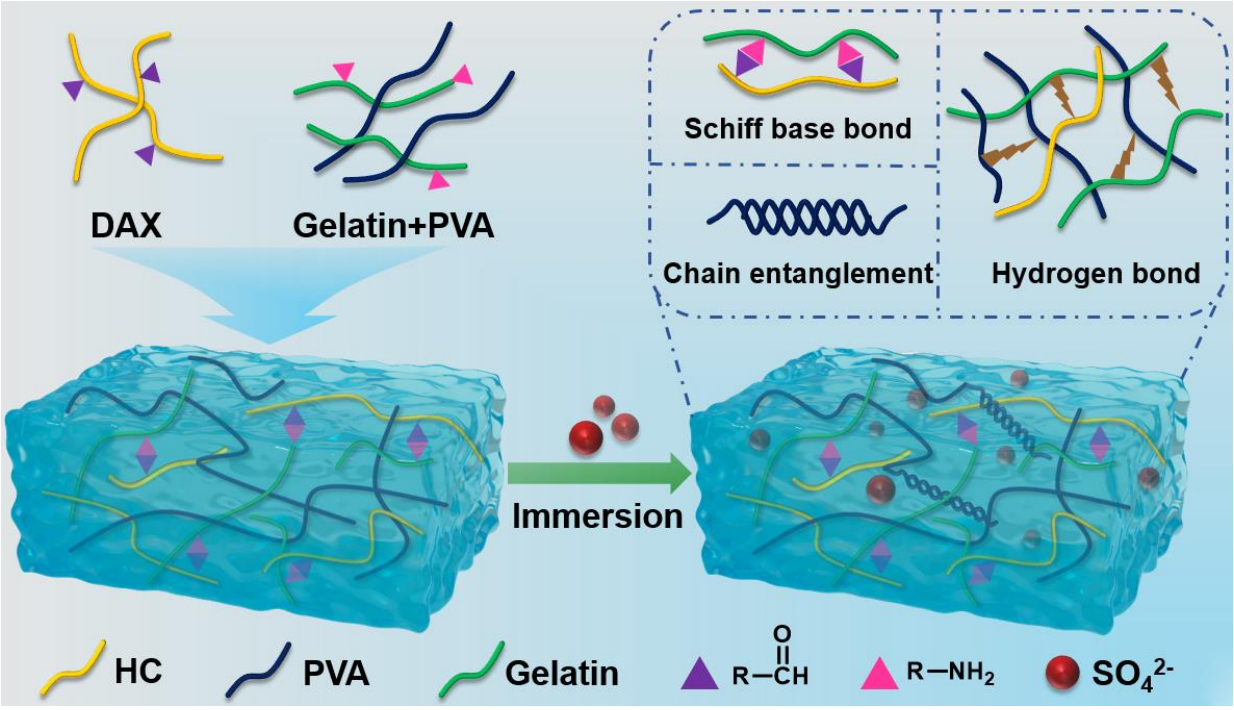

Fig. 1. Schematic of composite hydrogels fabrication

Micromorphology and Crystal-type Analysis

The H-PGD hydrogel shrunk considerably when soaked in Na_2SO_4 solution, as can be seen in Fig. 2a, and its size was reduced as SO_4^{2-} concentration increased. The morphology of composite hydrogels was examined through SEM (Fig. 2). The pictures show visible differences when comparing before and after Na_2SO_4 solution treatment. The network structure of the hydrogel was denser following treatment with Na_2SO_4 solution, as shown in Fig. 2 b through 2 d, and as concentration increased, the hydrogel's three-dimensional mesh structure progressively collapsed. The reason behind this is that SO_4^{2-} caused PVOH molecular chain entanglement contraction (Wu *et al.* 2021a). Following immersion treatment, the cross-section of composite hydrogel exhibited a uniform distribution of a noticeable amount of Na^+ and SO_4^{2-}, as demonstrated by the EDS analysis (Fig. 2f)

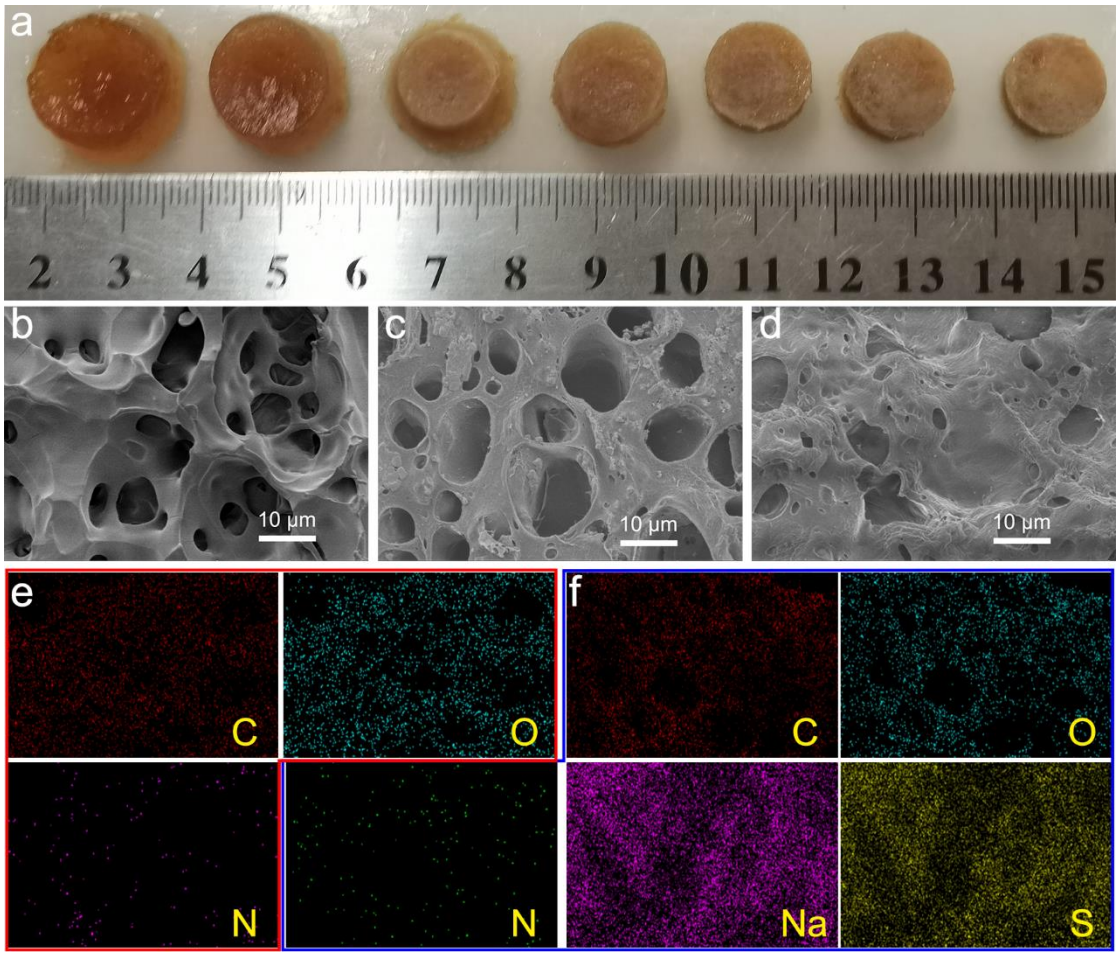

Fig. 2. (a) Images of composite hydrogels, including I-PGD and H-PGD hydrogels obtained by immersion 24 h in 40 mL 0.5, 1.0, 1.5, 2.0, 2.5, and 3.0 M Na_2SO_4 solution from left to right; SEM of (b) I-PGD composite hydrogel, (c) H-PGD composite hydrogel obtained by immersion 24 h in 40 mL 1 M Na_2SO_4 solution, (d) H-PGD composite hydrogel obtained by immersion 24 h in 40 mL 2 M Na_2SO_4 solution. DES mapping of (e) I-PGD composite hydrogel, (f) H-PGD composite hydrogel obtained by immersion 24 h in 40 mL 1 M Na_2SO_4 solution

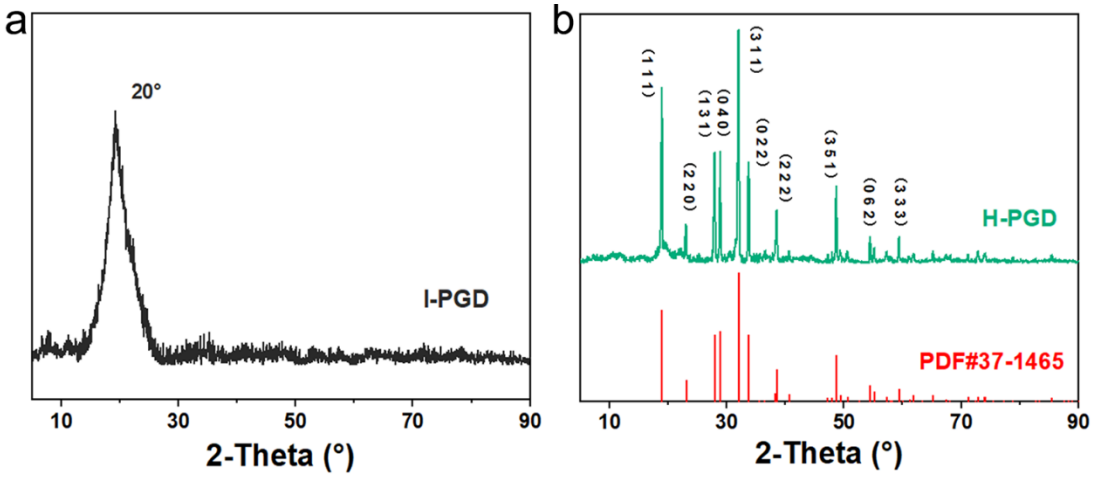

Fig. 3. XRD patterns of (a) I-PGD composite hydrogel and (b) H-PGD composite hydrogel obtained by immersed 24 h in 40 mL 1 M Na_2SO_4 solution

The XRD patterns of the composite hydrogels before and after a 24 h immersion in a 1 M Na_2SO_4 solution are displayed in Fig. 3. Prior to treatment, the composite hydrogel had a single broad diffraction peak near $2\theta = 20°$ and exhibited weak crystalline character. Following treatment, Na_2SO_4 diffused into the interior of the composite hydrogel as shown by the composite hydrogel's XRD pattern matching the PDF standard card for Na_2SO_4 (ICDD PDF No. 37-1465).

FT-IR Spectroscopy and XPS Analysis

The FT-IR spectra of HC and DAX zoomed in at the 1200 to 800 cm^{-1} range and full wavenumber range are displayed in Figs. 4a and 4b.

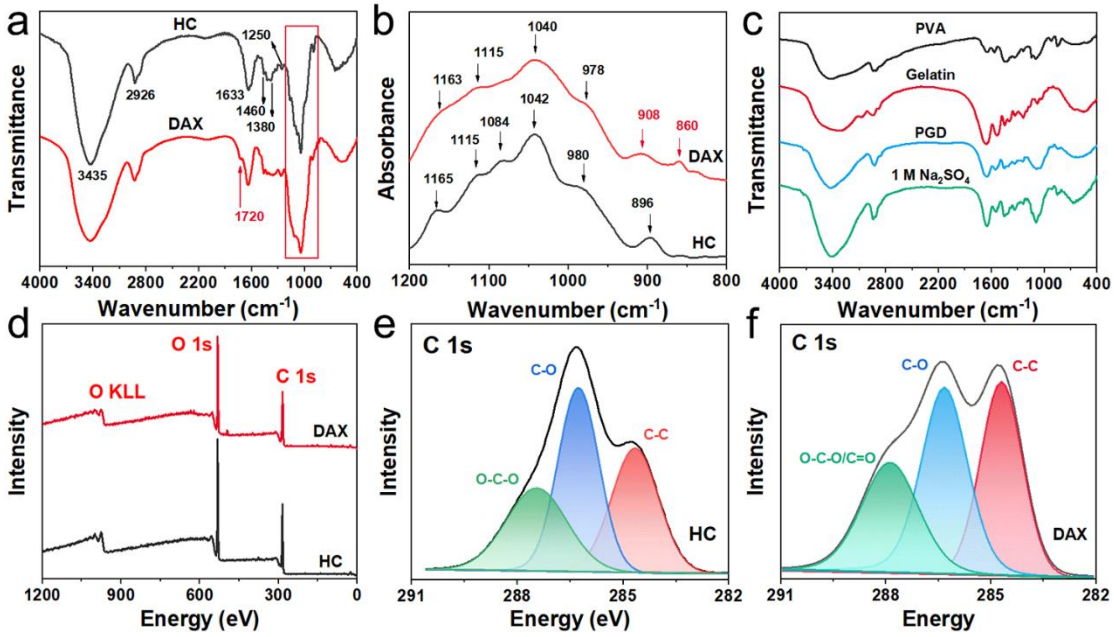

Fig. 4. FT-IR spectra of hemicellulose and DAX at (a) full wavenumber range, (b) zoomed in of the range between 1200 and 800 cm^{-1}. (c) FT-IR spectra of PVOH, gelatin, I-PGD composite hydrogel, and H-PGD composite hydrogel obtained by immersed 24 h in 40 mL 1 M Na_2SO_4 solution. XPS spectra of (d) full spectra, (e) HC C1s, and (f) DAX C1s

The peaks at 3435 and 2926 cm^{-1} are attributed to stretching vibrations of hydroxyl and methylene, respectively. The peak at 1635 cm^{-1} of HC is assigned to absorbed water. The peaks at 1165, 1087, and 1042 cm^{-1} are attributed to C-O, C-OH, and C-O-C contributions, respectively. The peaks at 1115 and 980 cm^{-1} are the characteristic absorption of arabinoxylan. The peak at 896 cm^{-1} is due to anomeric CH deformation of β-glycosidic linkage between the sugar units (Peng *et al.* 2012; Borovkova *et al.* 2022; Hu *et al.* 2022). Under the oxidation of $NaIO_4$, the FT-IR spectrum of DAX showed a new peak belonging to the aldehyde group at 1720 cm^{-1}. Apart from the peak at 909 cm^{-1} associated to the anomeric H in β-configuration, a characteristic peak at 858 cm^{-1} was attributed to hemialdal linkages formed from dialdehyde groups (Amer *et al.* 2016). After the process of gelation, the FT-IR spectra of I-PGD and H-PGD composite hydrogels exhibited distinct absorption bands that were associated with polysaccharides, primary amines, and PVOH. Notably, the aldehyde peak vanished due to the Schiff base reaction, while the intensity of the absorption bands related to primary amines was reduced.

An XPS survey spectrum was used to measure the HC and DAX surface O/C atomic ratio and the chemically bound state of C (Fig. 4a through 4c). Detailed data are listed in Table 1. In agreement with theory, the O/C atomic ratios of DAX and HC were nearly identical. The chemical binding state of C in DAX differs greatly from that of HC, though. Both HC and DAX's C1s spectra have three different values assigned to the C-C, C-O, and O-C-O/C=O structures, respectively: 284.7 eV, 286.3 eV, and 287.5 (287.9) eV (Li *et al.* 2009; Feng *et al.* 2022; Cheng *et al.* 2023). Comparing the DAX molecule to HC, the atomic concentration of C_2 was much lower, while the atomic concentration of C_3 was higher. It is evident from that oxidation reactions took place in the molecular structure of DAX, where some hydroxyl groups were changed into carbonyl groups.

Table 1. Summary of XPS Spectral Parameters of HC and DAX

Sample	C (%)	O (%)	O/C	C1s Component		Content (%)
HC	63.5	36.5	0.57	C_1	284.7 eV	31.7
				C_2	286.3 eV	42.9
				C_3	287.5 eV	25.4
DAX	64.2	35.8	0.56	C_1	284.7 eV	32.9
				C_2	286.3 eV	36.4
				C_3	287.9 eV	30.7

Mechanical Property

The I-PGD composite hydrogels had poor mechanical properties, which was expected because of the inherent nature of hemicellulose-based hydrogels. As determined by tensile testing, the tensile breaking strength was 29.4 kPa with an elongation on 80.3% of I-PGD composite hydrogels, and their compressive strength at 80% strain was only 0.57 MPa, as shown in Figs. 5 a, b. Conversely, under the impact of the Hofmeister effect, the mechanical properties of H-PGD were dramatically enhanced. The mechanical properties of the composite hydrogel were changed due to the ions' induction of polymer chain aggregation during salting out (Wu *et al*. 2021a). Through comparing the compressive strength under 80% strain and tensile properties of composite hydrogel in different anions, a typical Hofmeister series emerged following the sequence $SO_4^{2-} > S_2O_3^{2-} > H_2PO_4^- > CO_3^{2-} > CH_3COO^- > Cl^-$, with Na^+ as the constant counterion (Fig. 5 c, d). Additionally, the cationic salt solution was far less successful than the multivalent anions in strengthening the composite hydrogel when Cl^- was used as the counterion. K^+ and Na^+ were the two cationic salts with the greatest toughening effects out of the six that were chosen, each with a different valence. Among these, the composite hydrogel had a clear tendency toward salt dissolution as it gradually swelled to fragmentation under the soaking effects of Li^+, Ca^{2+}, and Fe^{3+} (Fig. 5 e, f).

Furthermore, the Hofmeister effect is usually concentration sensitive. Here, Na_2SO_4 was used as an example to study the influence of concentrations, due to its outstanding enhancement effect on the mechanical properties of composite hydrogels. The compressive strength of the H-PGD composite hydrogel rose with concentration, as Fig. 5e illustrates, and when the concentration was greater than 1.5 M, the compressive strength of the hydrogel surpassed 10 MPa. However, the H-PGD composite gel lost a considerable quantity of water due to the substantial aggregation of polymer chains when the concentration of the Na_2SO_4 solution surpassed 2 M. Additionally, the composite gel's compressive stress-strain curve gradually shifted from a "J" type to an "S" type curve. The tensile fracture strength of the H-PGD composite hydrogel is positively associated with the

concentration of SO_4^{2-}, as shown in Fig. 5 f; however, the elongation decreased noticeably as the concentration rose.

When combined with I-PGD, the H-PGD composite hydrogel had more extensive mechanical properties under the effect of 1 M SO_4^{2-}, showing a 10-fold increase in compression strength to 6.10 MPa. Concurrently, there was a notable enhancement in the tensile characteristics of the H-PGD composite hydrogel, exhibiting a tensile breaking strength of 3.02 MPa and an elongation of 331%. Furthermore, the composite hydrogels' compressive and tensile moduli were analyzed both before and after they were treated with Na_2SO_4 solution (Fig. 5). In contrast, H-PGD composite hydrogels showed increases in their compressive and tensile moduli of around approximately 220 and 60 times, respectively, reaching 1.82 MPa and 1.79 MPa.

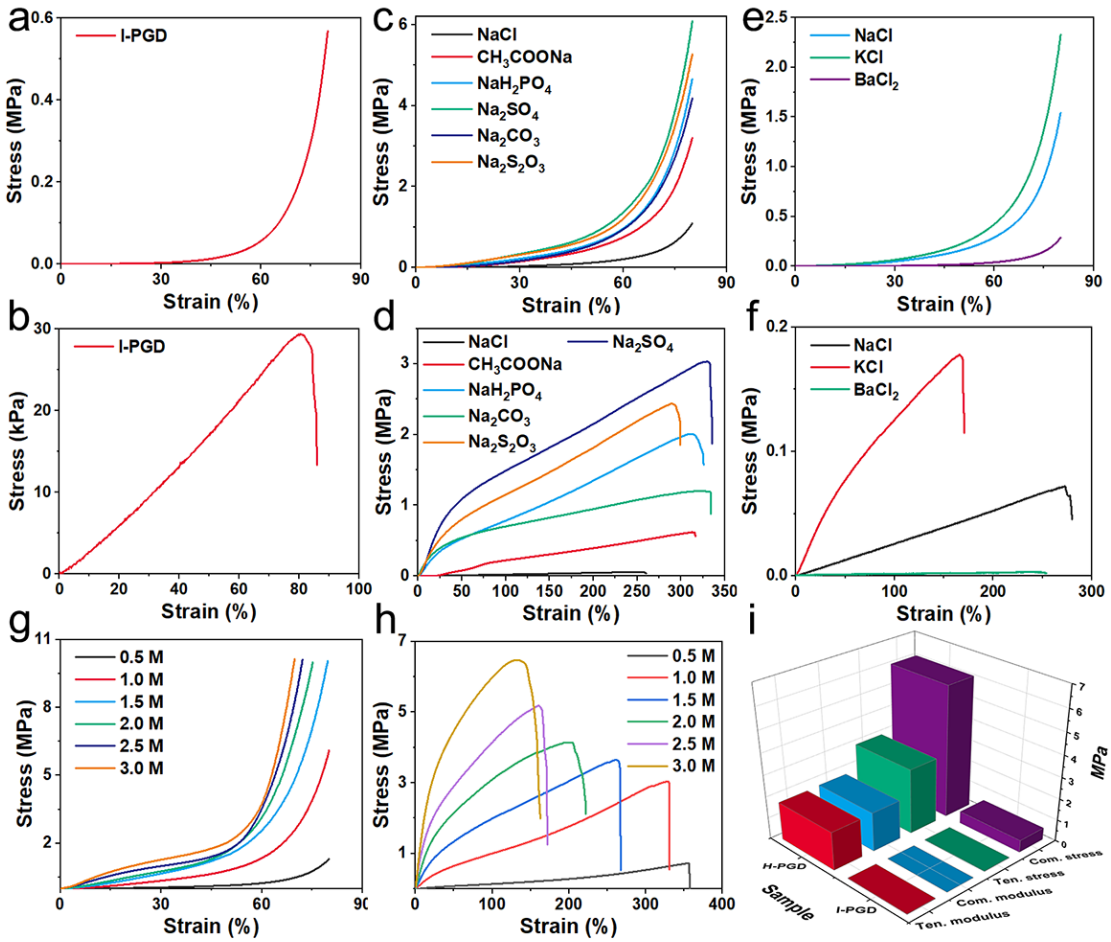

Fig. 5. Mechanical properties of different hydrogels: (a) compressive and (b) tensile stress-strain curves of I-PGD composite hydrogel, (c) compressive and (d) tensile stress-strain curves of H-PGD composite hydrogels after treatment with 1 M different anionic salt solutions, (e) compressive and (f) tensile stress-strain curves of H-PGD composite hydrogels after treatment with 1 M different cationic salt solutions, (g) compressive and (h) tensile stress-strain curves of H-PGD composite hydrogels after treatment with different Na_2SO_4 solution concentrations, (i) compressive stress, tensile stress, compressive stress and tensile stress of I-PGD composite hydrogel, and H-PGD composite hydrogel obtained by immersed 24 h in 1 M Na_2SO_4 solution

Electrochemical Performance

Both EDS and XRD analyses verified that Na^+ and SO_4^{2-} dispersed and stayed inside the hydrogel during the immersion process. As a result, the H-PGD composite hydrogel exhibited good ionic conductivity, which was demonstrated by subsequent experiments. The H-PGD hydrogel capacitor's schematic diagram is displayed in Fig. 6a. The hydrogel electrolyte's ability to store charge will be increased during the charging process when the electric field force transfers Na^+ and SO_4^{2-} from the hydrogel electrolyte to the electrodes. The H-PGD hydrogel capacitor is visible from the side in Fig. 6b, where the close integration of the hydrogel electrolyte and electrode material is evident. After that, a spreadsheet and LED lights were used to qualitatively test the H-PGD hydrogel capacitor's performance. The e-meter and LED light may be powered regularly by three fully charged H-PGD hydrogel capacitors connected in series, demonstrating their good multiplicity performance (Fig. 6 c, d).

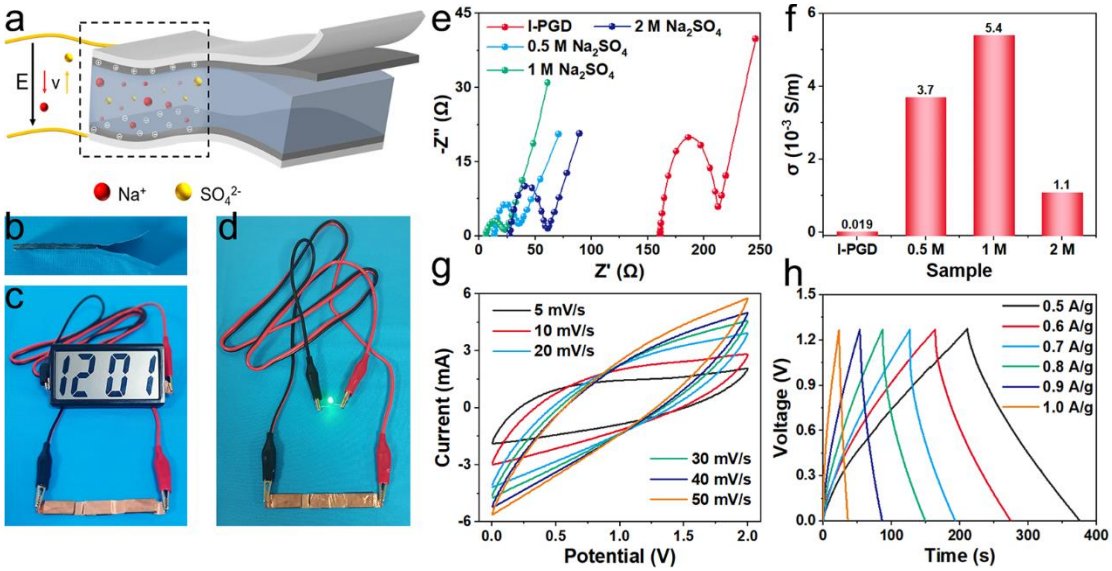

Fig. 6. (a) Schematic of H-PGD hydrogel capacitors, (b) Lateral photograph of H-PGD hydrogel capacitors, (c) Photograph of three H-PGD hydrogel capacitors in series for electronic meter power supply, (d) Photograph of three H-PGD hydrogel capacitors in series for powering LED, (e) -Nyquist diagram of hydrogel capacitors, (f) Ionic conductivity of composite hydrogels, (g) CV curve of H-PGD hydrogel capacitors, and (h) GCD curve of H-PGD hydrogel capacitors

An electrochemical workstation was used to further characterize the electrochemical properties of H-PGD hydrogel capacitors. The -Nyquist diagram shows that the I-PGD hydrogel capacitor had substantially greater contact and interfacial resistances than H-PGD (Fig. 6e). Concurrently, the hydrogel capacitor's resistance exhibited a trend of first reducing and then increasing when the concentration of the Na_2SO_4 solution rises. This is because at increased soaking concentrations, the higher the ion content, the more it diffused into hydrogel. In contrast, an excessively high ion concentration results in closely stacked polymer chains, which impacts ion transport inside the hydrogel (Wu *et al.* 2021b). Therefore, after soaking in a high concentration (2 M) of Na_2SO_4 solution, the H-PGD composite hydrogel's ionic conductivity was reduced. The H-PGD hydrogel's ionic conductivity may increase to 5.4×10^{-3} S/m during a 24 h immersion in a 1 M Na_2SO_4 solution, as illustrated in Fig. 6f.

Additionally, CV experiments were used to assess the electrochemical performance of H-PGD hydrogel capacitor. The hydrogel capacitor exhibited a voltage window of up to 2 V, as seen in Fig. 6g, and its double layer capacitive feature was indicated by the good symmetry of the CV curves at various voltage frequencies. Further mathematical calculations revealed that its electrode specific capacitance was 186.0 F/g. The charging and discharging curves of H-PGD hydrogel capacitors at various current densities, as seen in Fig. 6h, displayed symmetric triangles, demonstrating the quickness and reversibility of the electrochemical reaction. These imply that the H-PGD composite hydrogel may find use in super-capacitors.

CONCLUSIONS

In this work, a straightforward and effective process was developed for creating conductive composite hydrogels based on hemicellulose that have superior mechanical qualities. The hydrogel matrix was created by physically and chemically cross-linking polyvinyl alcohol (PVOH) and dialdehyde xylan (DAX) with gelatin. Additional reinforcement using Na_2SO_4 solution was then used to create the Hofmeister PVOH gelatin DAX (H-PGD) conductive composite hydrogel. After examining the composite hydrogels' mechanical, electrochemical, and structural characteristics, the following key findings were made.

1. A high-strength hemicellulose composite hydrogel was successfully prepared by soaking it in Na_2SO_4 solution with chemical and physical cross-linking based on DAX, gelatin, and PVOH. The tensile breaking strength and elongation of the H-PGD composite hydrogel increased to 3.02 MPa and 330.95%, after soaking for 24 h in the 1 M Na_2SO_4 solution. Additionally, it saw a factor of roughly 60 times to 1.79 MPa rise in its tensile modulus.
2. The denser cross-linked structure of the H-PGD composite hydrogel was formed as a result of the polymer chain aggregation caused by the salting-out effect, as validated by field emission SEM analysis. The XRD analysis and SEM-EDS mapping verified the diffusion and even distribution of Na^+ and SO_4^{2-} into the interior of the H-PGD composite hydrogel.
3. Using an electrochemical workstation, the H-PGD composite hydrogel's ionic conductivity was found to be 5.4×10^{-3} S/m. In contrast, H-PGD composite hydrogels can be used in super-capacitors, which have an electrode specific capacitance value of 186.0 F/g and a broad voltage window as well as good rate capability.

REFERENCES CITED

Amer, H., Nypelo, T., Sulaeva, I., Bacher, M., Henniges, U., Potthast, A., and Rosenau, T. (2016). "Synthesis and characterization of periodate-oxidized polysaccharides: Dialdehyde xylan (DAX)," *Biomacromolecules* 17(9), 2972-2980. DOI: 10.1021/acs.biomac.6b00777

Borovkova, V. S., Malyar, Y. N., Sudakova, I. G., Chudina, A. I., Zimonin, D. V., Skripnikov, A. M., Miroshnikova, A. V., Ionin, V. A., Kazachenko, A. S., Sychev, V.

V., *et al.* (2022). "Composition and structure of aspen (*Populus tremula*) hemicelluloses obtained by oxidative delignification," *Polymers (Basel)* 14(21), article ID 4521. DOI: 10.3390/polym14214521

Cheng, H., Fan, Z., Wang, Z., Guo, Z., Jiang, J., and Xie, Y. (2023). "Highly stretchable, fast self-healing nanocellulose hydrogel combining borate ester bonds and acylhydrazone bonds," *International Journal of Biological Macromolecules* 245, Article ID 125471. DOI: 10.1016/j.ijbiomac.2023.125471

Cui, W., Zheng, Y., Zhu, R., Mu, Q., Wang, X., Wang, Z., Liu, S., Li, M., and Ran, R. (2022). "Strong tough conductive hydrogels *via* the synergy of ion-induced cross-linking and salting-out," *Advanced Functional Materials* 32(39), article 4823. DOI: 10.1002/adfm.202204823

Dou, D., Wei, D., Guan, X., Liang, Z., Lan, L., Lan, X., Liu, P., Mo, H., and Lan, P. (2022). "Adsorption of copper (II) and cadmium (II) ions by *in situ* doped nano-calcium carbonate high-intensity chitin hydrogels." *Journal of Hazardous Materials* 423, article ID 127137. DOI: 10.1016/j.jhazmat.2021.127137

Elgueta, E., Becerra, Y., Martínez, A., Pereira, M., Carrillo-Varela, I., Sanhueza, F., Nuñez, D., and Rivas, B. L. (2023). "Adsorbents derived from xylan hemicellulose with removal properties of pollutant metals," *Chinese Journal of Polymer Science* 41(6), 874-886. DOI: 10.1007/s10118-023-2897-3

Feng, C., Zhu, J., Hou, Y., Qin, C., Chen, W., Nong, Y., Liao, Z., Liang, C., Bian, H., and Yao, S. (2022). "Effect of temperature on simultaneous separation and extraction of hemicellulose using p-toluenesulfonic acid treatment at atmospheric pressure," *Bioresource Technology* 348, article ID 126793. DOI: 10.1016/j.biortech.2022.126793

Fredricks, J. L., Jimenez, A. M., Grandgeorge, P., Meidl, R., Law, E., Fan, J., and Roumeli, E. (2023). "Hierarchical biopolymer-based materials and composites," *Journal of Polymer Science* 61(21), 2585-2632. DOI: 10.1002/pol.20230126

Gao, Y., Guo, M., Wang, D., Zhao, D., and Wang, M. (2023). "Advances in extraction, purification, structural characteristics and biological activities of hemicelluloses: A review," *International Journal of Biological Macromolecules* 225, 467-483. DOI: 10.1016/j.ijbiomac.2022.11.099

Gong, J. P., Katsuyama, Y., Kurokawa, T., and Osada, Y. (2003). "Double-network hydrogels with extremely high mechanical strength," *Advanced Materials* 15(14), 1155-1158. DOI: 10.1002/adma.200304907

Gong, Q., Li, Y., Liu, X., Xia, Z., and Yang, Y. (2020). "A facile preparation of polyaniline/cellulose hydrogels for all-in-one flexible supercapacitor with remarkable enhanced performance," *Carbohydrate Polymers* 245, article ID 116611. DOI: 10.1016/j.carbpol.2020.116611

Gutiérrez Hernández, J. M., Castorena Alejandro, C., Escobar García, D. M., Escalante, A., Flores, H., Pozos Guillen, A., Gatenholm, P., and Toriz, G. (2023). "*In vitro* evaluation of spruce xylan/MWCNTs hydrogel scaffolds for bone regeneration," *Materials Today Communications* 35, article ID 106070. DOI: 10.1016/j.mtcomm.2023.106 070

Haraguchi, K. (2011). "Synthesis and properties of soft nanocomposite materials with novel organic/inorganic network structures," *Polymer Journal* 43(3), 223-241. DOI: 10.1038/pj.2010.141

Hu, L., Xie, Y., Gao, S., Shi, X., Lai, C., Zhang, D., Lu, C., Liu, Y., Du, L., Fang, X., *et al.* (2023). "Strain-induced orientation facilitates the fabrication of highly stretchable

and tough xylan-based hydrogel for strain sensors," *Carbohydrate Polymers* 312, article ID 120827. DOI: 10.1016/j.carbpol.2023.120827

Hu, N., Chen, D., Guan, Q., Peng, L., Zhang, J., He, L., and Shi, Y. (2022). "Preparation of hemicellulose-based hydrogels from biomass refining industrial effluent for effective removal of methylene blue dye," *Environmental Technology* 43(4), 489-499. DOI: 10.1080/09593330.2020.1795930

Ihsan, A. B., Sun, T. L., Kurokawa, T., Karobi, S. N., Nakajima, T., Nonoyama, T., Roy, C. K., Luo, F., and Gong, J. P. (2016). "Self-healing behaviors of tough polyampholyte hydrogels," *Macromolecules* 49(11), 4245-4252. DOI: 10.1021/acs.macromol.6b00437

Jung, I. Y., Kim, J. S., Choi, B. R., Lee, K., and Lee, H. (2017). "Hydrogel based biosensors for *in vitro* diagnostics of biochemicals, proteins, and genes," *Advanced Healthcare Materials* 6(12), article ID 1601475. DOI: 10.1002/adhm.201601475

Lacroce, E., and Rossi, F. (2022). "Polymer-based thermoresponsive hydrogels for controlled drug delivery," *Expert Opinion on Drug Delivery* 19(10), 1203-1215. DOI: 10.1080/17425247.2022.2078806

Lee, H., You, J., Jin, H.-J., and Kwak, H. W. (2020). "Chemical and physical reinforcement behavior of dialdehyde nanocellulose in PVA composite film: A comparison of nanofiber and nanocrystal," *Carbohydrate Polymers* 232, article ID 115771. DOI: 10.1016/j.carbpol.2019.115771

Lee, K. Y., and Mooney, D. J. (2001). "Hydrogels for tissue engineering," *Chemical Reviews* 101(7), 1869-1880. DOI: 10.1021/cr000108x

Li, J., Chee, H. L., Chong, Y. T., Chan, B. Q. Y., Xue, K., Lim, P. C., Loh, X. J., and Wang, F. (2022a). "Hofmeister effect mediated strong PHEMA-gelatin hydrogel actuator," *ACS Applied Materials & Interfaces* 14(20), 23826-23838. DOI: 10.1021/acsami.2c01922

Li, J., Wan, Y., Li, L., Liang, H., and Wang, J. (2009). "Preparation and characterization of 2,3-dialdehyde bacterial cellulose for potential biodegradable tissue engineering scaffolds." *Materials Science and Engineering: C* 29(5), 1635-1642. DOI: 10.1016/j.msec.2009.01.006

Li, X., and Gong, J. P. (2024). "Design principles for strong and tough hydrogels," *Nature Reviews Materials* 9, 380-398. DOI: 10.1038/s41578-024-00672-3

Li, X., Liu, Z., Liang, Y., Wang, L.-M., and Liu, Y. D. (2022b). "Chitosan-based double cross-linked ionic hydrogels as a strain and pressure sensor with broad strain-range and high sensitivity," *Journal of Materials Chemistry B* 10(18), 3434-3443. DOI: 10.1039/D2TB00329E

Li, Y., Yao, M., Luo, Y., Li, J., Wang, Z., Liang, C., Qin, C., Huang, C., and Yao, S. (2023). "Polydopamine-reinforced hemicellulose-based multifunctional flexible hydrogels for human movement sensing and self-powered transdermal drug delivery," *ACS Applied Materials & Interfaces* 15(4), 5883-5896. DOI: 10.1021/acsami.2c19949

Lin, S., Liu, X., Liu, J., Yuk, H., Loh, H.-C., Parada, G. A., Settens, C., Song, J., Masic, A., and McKinley, G. H. (2019). "Anti-fatigue-fracture hydrogels," *Science Advances* 5(1), article ID eaau8528. DOI: 10.1126/sciadv.aau8528

Ling, Z., Ma, J., Zhang, S., Shao, L., Wang, C., and Ma, J. (2022). "Stretchable and fatigue resistant hydrogels constructed by natural galactomannan for flexible sensing application," *International Journal of Biological Macromolecules* 216, 193-202. DOI: 10.1016/j.ijbiomac.2022.06.185

Mondal, A. K., Xu, D., Wu, S., Zou, Q., Huang, F., and Ni, Y. (2022). "Design of Fe^{3+}-rich, high-conductivity lignin hydrogels for supercapacitor and sensor applications," *Biomacromolecules* 23(3), 766-778. DOI: 10.1021/acs.biomac.1c01194

Okumura, Y., and Ito, K. J. A. m. (2001). "The polyrotaxane gel: A topological gel by figure-of-eight cross-links," 13(7), 485-487. DOI: 10.1002/1521-4095(200104)13:7<485::AID-ADMA485>3.0.CO;2-T

Pan, X., Li, J., Ma, N., Ma, X., and Gao, M. (2023). "Bacterial cellulose hydrogel for sensors," *Chemical Engineering Journal* 461, article ID 142062. DOI: 10.1016/j.cej.2023.142062

Peng, X., Ren, J., Zhong, L., Sun, R., Shi, W., and Hu, B. (2012). "Glycidyl methacrylate derivatized xylan-rich hemicelluloses: Synthesis and characterizations," *Cellulose* 19(4), 1361-1372. DOI: 10.1007/s10570-012-9718-0

Qi, X. M., Chen, G. G., Gong, X. D., Fu, G. Q., Niu, Y. S., Bian, J., Peng, F., and Sun, R. C. (2016). "Enhanced mechanical performance of biocompatible hemicelluloses-based hydrogel *via* chain extension," *Scientific Reports* 6, article ID 33603. DOI: 10.1038/srep33603

Rao, J., Lv, Z., Chen, G., and Peng, F. (2023). "Hemicellulose: Structure, chemical modification, and application," *Progress in Polymer Science* 140, article ID 101675. DOI: 10.1016/j.progpolymsci.2023.101675

Sarmah, D., and Karak, N. (2022). "Starch based mechanically tough hydrogel for effective removal of toxic metal ions from wastewater," *Journal of Cleaner Production* 344, article ID 131074. DOI: 10.1016/j.jclepro.2022.131074

Song, Y., Niu, L., Ma, P., Li, X., Feng, J., and Liu, Z. (2023). "Rapid preparation of antifreezing conductive hydrogels for flexible strain sensors and supercapacitors," *ACS Applied Materials & Interfaces* 15(7), 10006-10017. DOI: 10.1021/acsami.2c21617

Sun, X. F., Liu, B., Jing, Z., and Wang, H. (2015). "Preparation and adsorption property of xylan/poly(acrylic acid) magnetic nanocomposite hydrogel adsorbent," *Carbohydrate Polymers* 118, 16-23. DOI: 10.1016/j.carbpol.2014.11.013

Tsay, K.-C., Zhang, L., and Zhang, J. (2012). "Effects of electrode layer composition/thickness and electrolyte concentration on both specific capacitance and energy density of supercapacitor," *Electrochimica Acta* 60, 428-436. DOI: 10.1016/j.electacta.2011.11.087

Wang, Z., Shu, L., Zhang, X.-F., and Yao, J. (2023). "Double cross-linked wood hydrogels with high anisotropy and ionic conductivity for sensitive pressure sensing," *Colloids Surfaces A: Physicochemical Engineering Aspects* 658, article ID 130688.

Wichterle, O., and Lim, D. (1960). "Hydrophilic gels for biological use," *Nature* 185(4706), 117-118. DOI: 100.1038/185117a0

Wu, S., Hua, M., Alsaid, Y., Du, Y., Ma, Y., Zhao, Y., Lo, C. Y., Wang, C., Wu, D., Yao, B., *et al.* (2021a). "Poly(vinyl alcohol) hydrogels with broad-range tunable mechanical properties *via* the Hofmeister Effect," *Advance Materials* 33(11), article ID e2007829. DOI: 10.1002/adma.202007829

Wu, Y., Mu, Y., Luo, Y., Menon, C., Zhou, Z., Chu, P. K., and Feng, S. P. (2021b). "Hofmeister effect and electrostatic interaction enhanced ionic conductive organohydrogels for electronic applications," *Advanced Functional Materials* 32(15), article ID 2110859. DOI: 10.1002/adfm.202110859

Yin, C., Huang, Z., Zhang, Y., Ren, K., Liu, S., Luo, H., Zhang, Q., and Wan, Y. (2024). "Strong, tough, and elastic poly(vinyl alcohol)/polyacrylamide DN hydrogels based

on the Hofmeister effect for articular cartilage replacement," *Journal of Materials Chemistry B* 12(12), 3079-3091. DOI: 10.1039/d3tb02637j

Yu, Z., Li, Q., He, X., Wang, X., Wen, Y., Zeng, L., and Chen, H. (2023). "A multifunctional hydrogel based on nature polysaccharide fabricated by Schiff base reaction," *European Polymer Journal* 197, article 112330. DOI: 10.1016/j.eurpolymj.2023.112330

Yuan, X., Zhu, Z., Xia, P., Wang, Z., Zhao, X., Jiang, X., Wang, T., Gao, Q., Xu, J., and Shan, D. (2023). "Tough gelatin hydrogel for tissue engineering," *Advanced Science* 10(24), article ID 2301665. DOI: 10.1002/advs.202301665

Zhao, X., Chen, X., Yuk, H., Lin, S., Liu, X., and Parada, G. (2021). "Soft materials by design: Unconventional polymer networks give extreme properties," *Chemical Reviews* 121(8), 4309-4372. DOI: 10.1021/acs.chemrev.0c01088

Zhou, W., Duan, Z., Zhao, J., Fu, R., Zhu, C., and Fan, D. (2022). "Glucose and MMP-9 dual-responsive hydrogel with temperature sensitive self-adaptive shape and controlled drug release accelerates diabetic wound healing," *Bioactive Materials* 17, 1-17. DOI: 10.1016/j.bioactmat.2022.01.004

Zou, H., Meng, X., Zhao, X., and Qiu, J. (2023). "Hofmeister effect-enhanced hydration chemistry of hydrogel for high-efficiency solar-driven interfacial desalination," *Advanced Materials* 35(5), article ID e2207262. DOI: 10.1002/adma.202207 262

Article submitted: June 5, 2024; Peer review completed: June 30, 2024; Revised version received and accepted: July 7, 2024; Published: August 29, 2024.
DOI: 10.15376/biores.19.4.7708-7722